www.sciencemag.org/cgi/content/full/science.1222538/DC1

Supplementary Material for

Cilia at the Node of Mouse Embryos Sense Fluid Flow for Left-Right Determination via Pkd2

Satoko Yoshiba, Hidetaka Shiratori, Ivana Y. Kuo, Aiko Kawasumi, Kyosuke Shinohara, Shigenori Nonaka, Yasuko Asai, Genta Sasaki, Jose Antonio Belo, Hiroshi Sasaki, Junichi Nakai, Bernd Dworniczak, Barbara E. Ehrlich, Petra Pennekamp,* Hiroshi Hamada*

*To whom correspondence should be addressed. E-mail: petra.pennekamp@uni-muenster.de (P.P.); hamada@fbs.osaka-u.ac.jp (H.H.)

Published 13 September 2012 on *Science* Express
DOI: 10.1126/science.1222538

This PDF file includes:

Other Supplementary Material for this manuscript includes the following:
(available at www.sciencemag.org/cgi/content/full/science.1222538/DC1)

Movies S1 to S3

Supporting Online Materials (Yoshiba et al)

Materials and Methods

Transgene constructs

For the generation of a transgene that confers expression of *Pkd2* in the node, mouse *Pkd2* cDNA was linked to *IRES-LacZ* (an internal ribosome entry site linked to the β-galactosidase gene) and placed under the control of a 1.5kb DNA fragment of the node/notochord specific enhancer of the mouse *Foxa2* gene(*1*) and the mouse *Hsp68* promoter. For pit cell specific expression of Pkd2, the node/notochord-specific enhancer of dwarf gourami *Foxa2* gene(*2*) was used. For the generation of transgenes that are expressed specifically in crown cells, mouse *Pkd2*, *Pkd2::$(G_4S)_3$-Venus*(*3*), or *Kif3a* cDNA was linked (or not) to *IRES-LacZ* and placed under the control of two tandem copies of a 0.7-kb DNA fragment of the node-specific enhancer (NDE) of mouse *Nodal*(*4, 5*) and the *Hsp68* promoter. Point mutagenesis of *Pkd2* was performed with the use of a Mutan-Express Km system (Takara). The mutagenesis primers included 5'-GCTGCGGCTGCACGC**C**TCTGGAGTTAACCATG-3' (R6G), 5'-CCCGTTGCTGGGAACC**C**CGCCAATAACCTGAC-3' (E442G) and 5'-ACGACAATCACAACA**A**CCAGACAATTCCAGAAAC-3' (D509V), with the mutated nucleotides shown in bold and underlined. The COOH-terminal truncation construct *Pkd2*(*G819X*) was produced by introducing a stop codon at the codon for glycine-819. *Pkd2*(Δ5–73) construct was generated by PCR mutagenesis as previously described(*6*). *Pkd2* bacterial artificial chromosome (BAC) transgene (*Pkd2-LacZ/BAC*) was constructed with BAC clone (RP24-3271I4) containing mouse *Pkd2*. *IRES-LacZ*

was inserted in the 3' untranslated region of *Pkd2*, as previously described.

Mice

Pkd2$^{-/-}$ and *Cerl2*$^{-/-}$ mice were previously described(*7, 8*). *Kif3a*$^{+/-}$ mouse was purchased from The Jackson Laboratory (Strain Name: B6.129-Kif3a<tm1Gsn>/J). For the generation of transgenic mice, each transgene (*Tg*) was microinjected into the pronucleus of fertilized eggs obtained by crossing C57BL/6J female with *Pkd2*$^{+/-}$ or *Kif3a*$^{+/-}$ male mice. To obtain *Pkd2*$^{-/-}$;*Tg*$^{+}$ (or *Kif3a*$^{-/-}$, *Tg*$^{+}$) embryos, we mated *Pkd2*$^{+/-}$ (or *Kif3a*$^{-/-}$) females with *Pkd2*$^{+/-}$;*Tg*$^{+}$ (or *Kif3a*$^{+/-}$, *Tg*$^{+}$) males. Mice and embryos were genotyped by the polymerase chain reaction. Primers for the detection of *Pkd2* cDNA were 5'-GGGGAACAAGACTCATGGAA-3' (exon 2) and 5'-ACACTGGGGTGTCTATGAAT-3' (exon 3). Transgenic lines were screened for node-specific expression by X-gal (5-bromo-4-chloro-3-indolyl-β-D-galactopyranoside) staining of whole embryos. Node-specific expression was further confirmed by staining with paraffin-embedded sections. Transgenic mouse harboring *ANE-LacZ,* in which *LacZ* expression is driven by the 7.5 kb upstream region of the human *Lefty1* gene, was previously described(*9*).

Whole-mount *in situ* hybridization

Whole-mount *in situ* hybridization was performed according to standard procedures with digoxigenin-labeled riboprobes specific for *Nodal*, *Pitx2*, *Gdf1*, *Cerl2*, *LacZ,* and *Venus*.

Immunofluorescence analysis

E8.0 mouse embryos were dissected, fixed in 4% paraformaldehyde, and dehydrated in

methanol. They were then permeabilized with 0.1% Triton X-100 in phosphate-buffered saline, exposed to TNB Blocking Buffer (TSA System), and finally incubated first with primary antibodies and then with Alexa Fluor-conjugated secondary antibodies. Primary antibodies included: rabbit polyclonal anti-Pkd2 (YCB9), rabbit polyclonal anti-green fluorescent protein (MBL; for detection of Venus), mouse monoclonal anti-acetylated tubulin (Sigma), chicken polyclonal anti-β-galactosidase (Abcam), and rat monoclonal anti-E-cadherin (ECCD-2, Takara). Some embryos were also stained with Alexa Fluor 633-conjugated phalloidin to detect F-actin. The nodes of stained embryos were excised, placed on slide glasses with silicone rubber spacers, covered with cover glasses, and imaged with Olympus FV1000 confocal microscope.

Measurement of nodal flow and ciliary motility

For visualization of nodal flow, fluorescent microbeads (diameter, 0.2 μm; Invitrogen) were applied to the node, and the positions of the beads were traced for 10 s (30 frames per second). Time-series images were subjected to PIV analysis as previously described(*10, 11*). The cilia of crown cells were labeled with the use of the *NDE-Pkd2::Venus* transgene and visualized with a Leica confocal microscope (DMI6000B) equipped with a CSU-Xl confocal unit (Yokogawa) and iXon EMCCD camera (Andor Technology). To count the number of motile cilia in crown cells, fluorescence of Venus was monitored for 10 s (30 frames per second). Time-series images were stacked and processed by Average Intensity projection with ImageJ software (NIH). To estimate the number of motile cilia in the pit cells, we used a high-speed CMOS camera (HAS-500M, Detect, 100 frames/s) connected to an Axiovert

100M microscope (Zeiss). To visualize the outline of nodal cilia, we first subtracted the average image from the time-series images and enhanced contrast with 0.5% saturated pixels by ImageJ.

Cell culture, transfection and microsome preparation

LLC-PK1 cells were maintained with M199 medium-3% fetal bovine serum. For analysis of cilia, cells were grown for up to 1week post confluence. Pkd2 expression vectors for stable cell lines were constructed in pEFSA/neo or pEFSA/puro. Transfections were performed with Lipofectamine 2000 (Invitrogen). Cells were selected 24 hours after transfection with 1μg/ml Puromycin or 400μg/ml G418 for 2 weeks. Cell lines highly expressing Pkd2 were selected by immunoblotting with YCB9 antibody. Membrane vesicles enriched for endoplasmic reticulum (ER) were prepared as previously described(*12*).

Single Channel Recording

ER microsomes enriched with Pkd2(wt), Pkd2(E442G) or Pkd2(R6G,G819X) were fused to lipid bilayers. Experiments were performed with 250 mM HEPES-Tris solution (pH 7.35) on the *cis* and 250 mM HEPES, 55 mM $Ba(OH)_2$ solution (pH 7.35) on the *trans* side. Pkd2 channels were activated by the addition of Ca^{2+} to the *cis* side. Channel activity was recorded for 2 min at each Ca^{2+} concentration under voltage-clamp conditions on a Bilayer Clamp BC-525C (Warner Instuments, Hartford, CT, USA), filtered at 1 kHz and digitized at 5 kHz. Data was acquired and analyzed with pClamp9 (Axon Instruments, Burlingame, CA).

Co-immunoprecipitation

An expression vector for 3xMyc-tagged Pkd2 was constructed in BOS-EX(*13*). An expression vector for GFP-tagged C-terminal Pkd1l1 (Pkd1l1-CC-GFP) is a gift from DP. Norris(*14*). Transfection to HEK293T cells was performed with Lipofectamine 2000 (Invitrogen). Cells were collected 12hr after transfection, and were lysed in RIPA buffer [50mM Tris-HCl, 150mM sodium chloride, 0.5% sodium deoxycholate, 0.1% SDS and 1% Nonidet P-40, 1mM EDTA and the complete protease inhibitor cocktail (Roche)]. The cleared cell lysate was incubated with a polyclonal anti-GFP antibody (MBL) bound to Dyna Protein G beads (Invitrogen) for 1 hour, and bound proteins were then eluted with laemmli buffer. The eluted proteins were subjected to polyacrylamide gel electrophoresis (6% for Pkd2-3xMyc; 10% for Pkd1l1-CC-GFP) followed by Western blot analysis with a monoclonal antibody against c-Myc (9E10; Santa Cruz) or a monoclonal antibody against GFP (Clontech).

Mouse embryo Culture

Embryos were collected at E7.5. Embryos at the early headfold (EHF) stage were selected and were cultured with 75% rat serum/ DMEM under 5% CO_2 at 37°C. Inhibitors were added to the medium at the final concentration of 500μM $GdCl_3$, 100μM 2-aminoethoxydiphenyl borate, 1μM Ruthenium Red or 500nM Tharpsigargin. For Thapsigargin, embryos were cultured with the reagent for initial 30min, and were cultured without Thapsigargin for the rest of the time. Embryo culture with artificial fluid flow was performed as described previously(*15*).

Scanning electron microscopy

Embryos were dissected, fixed with 1% glutaraldehyde in phosphate-buffered saline,

and treated with 1% OsO_4 in phosphate-buffered saline. They were then dehydrated, freeze-dried (ES-2030, Hitachi), and coated with platinum by ion sputtering (E-1010, Hitachi) for observation with a scanning electron microscope (S-2600N, Hitachi).

Introduction of expression vectors into the LPM

Expression vectors were introduced to the LPM by lipofection, as we described previously(*16*).

GCaMP2 Ca^{2+} imaging

GCaMP2 transgene was linked to *IRES-LacZ* and placed under the control of *NDE* enhancer to be expressed specifically in crown cells. Embryos carrying *GCaMP2* transgenes were collected in 10%FBS/DMEM/Hepes (pH7.2). Distal portions including the node cavity were dissected, placed onto a slide glass with a silicone rubber spacer and covered with a thin glass (0.17mm). 40×objective lens (HCX PL APO, Leica) was used for imaging. GCaMP2 was excited at 488nm and visualized with a Leica confocal microscope (DMI6000B) equipped with a CSU-Xl confocal unit (Yokogawa) and iXon EMCCD camera (Andor Technology). Data were processed and analyzed by ImageJ. Z-series images were stacked by Max Intensity projection and pseudo-colored. To compare the signal intensity in left crown cells (F_{left}) with that in right crown cells (F_{right}), signal intensity in each crown cell region of individual embryos was averaged. Statistical analyses were performed with student's *t*-test, and *p* values <0.05 were considered as significantly different.

Legends to Supplementary Figures

Figure S1. Ubiquitous expression of *Pkd2* in the mouse embryo.

(A) Whole-mount *in situ* hybridization analysis of *LacZ* expression in $Pkd2^{+/+}$ and $Pkd2^{LacZ/LacZ}$ embryos, the latter of which harbor *LacZ* at the *Pkd2* locus(*7*), at embryonic day E7.5. Lateral views are shown for both embryos, whereas a ventral view is also shown for the latter embryo. Note that *LacZ* mRNA is present ubiquitously in the $Pkd2^{LacZ/LacZ}$ embryo. Scale bar, 50μm. (**B**) Staining for β-galactosidase (β-gal) with the substrate X-gal in E7.5 embryos without (Tg^-) or with (Tg^+) a *Pkd2* bacterial artificial chromosome transgene (*Pkd2 BAC-IZ Tg*), in which *IRES-LacZ* is inserted in the 3' untranslated region of *Pkd2*. Whole-embryo views are shown for Tg^- and Tg^+ embryos. A high-magnification view of the node and a transverse section are shown for the Tg^+ embryo. Node is outlined with white line in the high-magnification view and indicated by arrowhead in the transverse section. Scale bars, 50μm.

Figure S2. The LPM of the $Pkd2^{-/-}$ embryo is competent to Nodal signaling.

An expression vector for Nodal and an EGFP expression vector were co-injected into the prospective right LPM of $Pkd2^{+/+ \text{ or } +/-}$ and $Pkd2^{-/-}$ embryos at the early headfold stage. The site of injection was confirmed by the fluorescence of EGFP (white arrowhead). Injected embryos were cultured for 14hr and then subjected to *in situ* hybridization for *Nodal*. Note that expression of endogenous *Nodal* gene was induced in the entire right LPM of $Pkd2^{+/+,+/-}$ and $Pkd2^{-/-}$ embryos. Scale bar, 500μm. The numbers of embryos showing each pattern of gene expression are summarized at the bottom.

Figure S3. Pit cell-specific rescue of Pkd2 does not restore normal L-R determination.

(**A**) A ventral view of the node in an E8.0 embryo obtained by scanning electron microscopy is shown in left panel. A, anterior; P, posterior; L, left; R, right. The region boxed by black lines represents the plane of the schematic sectional view shown in right panel. Yellow, endoderm; grey, mesoderm; green, ectoderm; light purple, node pit cells; dark purple, node crown cells. The blue arrow in the mesoderm on the left indicates the route of Nodal signal transmission from node to left LPM. **(B, C**) Pkd2 expression in pit cells is not sufficient for correct L-R determination. (**B**) Transgenic mouse showing pit cell-specific expression of *Pkd2*. *Pkd2-IRES-LacZ* was driven by two tandem copies of the node/notochord enhancer of *Foxa2* gene from fish, dwarf gourami (*dgFoxa2*) (*2*). Expression pattern was examined by staining embryos with X-gal. Views of whole embryos (left), the node at higher magnification (middle) and transverse sections of the node (right) are shown. White lines (middle) indicate the border between the endoderm and crown cells, with the dotted circle enclosing pit cells. Scale bars, 50μm. (**C**) Expression of *Nodal* and *Pitx2* in *Pkd2*$^{-/-}$ embryo with *dgFoxa2-Pkd2* transgene, showing that pit cell-specific expression of *Pkd2* is unable to rescue laterality defect of *Pkd2*$^{-/-}$. Red arrowheads indicate bilateral expression of *Pitx2*. Scale bar, 500μm. (**D**) Summary of *Nodal* and *Pitx2* expression patterns in E8.0 embryos of the indicated genotypes. The numbers of embryos examined are indicated.

Figure S4. *Cerl2* is the major target of Pkd2-mediated signaling in crown cells.

(A) Expression of *Gdf1*, *Cerl2*, and *Nodal* in crown cells of *Pkd2*$^{+/+}$ and *Pkd2*$^{-/-}$ embryos at E8.0. Whereas bilateral *Gdf1* expression is maintained in the *Pkd2*$^{-/-}$ mutant, L-R asymmetric expressions of *Cerl2* and *Nodal* are disrupted, notably that of *Cerl2* is not down-regulated at left side as *Pkd2*$^{+/+}$ (red arrowheads). Scale bar, 50μm. (**B**) Representative expression patterns of *Nodal* in wild-type, *Pkd2*$^{-/-}$, *Cerl2*$^{-/-}$, and *Pkd2*$^{-/-}$;*Cerl2*$^{-/-}$ embryos at E8.0. Green and orange arrowheads indicate expression in the right and left LPM, respectively. The phenotype of *Pkd2*$^{-/-}$;*Cerl2*$^{-/-}$ mutant was similar to that of the *Cerl2*$^{-/-}$ mutant. Scale bar, 500μm. **(C**) Summary of *Nodal* expression patterns in LPM for E8.0 embryos of the indicated genotypes. The numbers of embryos examined are indicated. **(D**) Model for the role of Pkd2. In crown cells on the right, Cerl2 inhibits Nodal and prevents the Nodal signal from being transmitted to LPM. On the left side, an unknown Pkd2-mediated signal suppresses *Cerl2* expression in a flow-dependent manner, resulting in up-regulation of Nodal activity. In parallel, Pkd2 may promote the Nodal signal by a different mechanism (dotted line) not dependent on Cerl2.

Figure S5. The node and node cilia are morphologically normal in *Pkd2*$^{-/-}$ embryos. The node of *Pkd2*$^{+/+}$ (upper) and *Pkd2*$^{-/-}$ (lower) embryos at E8.0 was examined by scanning electron microscopy. The boxed regions on the left are shown at higher magnification on the right. Scale bars, 5 μm.

Figure S6. Crown cells do not show obvious L-R asymmetry in Ca^{2+} signals.

Transgenic mouse expressing a Ca^{2+} indicator GCaMP2 in crown cells was generated with *NDE-hsp-GCaMP2-IRES LacZ*. Crown cells of transgenic embryos were examined for Ca^{2+} signaling. The fluorescence intensity did not differ between left and right crown cells, both in *Pkd2*$^{+/+,+/-}$ (P=0.382, n=11) and *Pkd2*$^{-/-}$ (P=0.438, n=3) (upper). Data are shown as the ratio of signal intensity in left crown cells vs. that in right crown cells (F_{left}/F_{right}). Bars represent ± SEM. Representative fluorescence images and expression of GCaMP2 protein (as revealed by immunofluorescence with anti-GFP antibody) are shown for *Pkd2*$^{+/-}$ (lower left) and *Pkd2*$^{-/-}$ (lower right), respectively. Signal intensity is represented by pseudocolor (red>yellow>blue). Note that the level of Ca^{2+} signaling in crown cells is not saturated. Scale bars, 20μm.

Figure S7. The net level of intracellular Ca^{2+} signal in crown cells does not change significantly by treatment with Thapsigargin.

Transgenic embryos expressing GCaMP2 in crown cells that were not treated with Thapsigargin (A) or treated with 1μM Thapsigargin for 30 minutes (B) were examined for fluorescence intensity. Note that F_{left}/F_{right} in control culture (P=0.565, n=4) was not changed after treatment with Thapsigargin (P=0.509, n=4). Bars represent ± SEM. Signal intensity is represented by pseudocolor (red>yellow>blue). Scale bar, 50 μm.

Figure S8. Ciliary localization of Pkd2::Venus is not altered by Ca^{2+} signal inhibitors.

Transgenic embryos expressing Pkd2::Venus in crown cells were collected at E7.5 and

cultured for 3hours or 12hours with 250μM Gd^{3+} or 1μM Thapsigargin. Localization of Pkd2::Venus was examined by Venus fluorescence. Note that ciliary localization of Pkd2::Venus remained after treatment with these inhibitors. Scale bar, 10μm.

Figure S9. Sub-cellular localization of various Pkd2 mutants in the node crown cells.

(A) Endogenous Pkd2 localized to the cilia of crown cells. Immunofluorescence staining of E8.0 wild-type embryo for Pkd2 (green), acetylated tubulin (red), and E-cadherin (cyan). Scale bar, 10 μm. **(B-D)** Ability of mutant forms of Pkd2 to localize to crown cell cilia. E8.0 embryos expressing the indicated transgenes were stained with antibodies to Pkd2 (green), to acetylated tubulin (red), and to β-galactosidase (cyan) (**B**), or with antibodies to Venus; GFP (red), antibodies to acetylated tubulin (green), and phalloidin (cyan) (**C, D**). Ciliary localization is maintained for Pkd2(R6G) (**B**) and Pkd2(Δ5–73) (**C**), but not for Pkd2(R6G, G819X) (**D**). Scale bars, 10μm.

Figure S10. Motility of cilia in crown cells and pit cells.

(A) Motility of cilia in crown cells and pit cells was examined as described in Materials and Methods. To examine motility of crown cell cilia, time-series images of Venus fluorescence (300 frames) were stacked for transgenic embryos harboring *NDE-hsp-Pkd2::Venus -IRES LacZ*, at the presomite (EHF) and three-somite (3 somote) stages. Motile and immotile cilia are shown in red and blue, respectively. Scale bar, 10 μm. **(B)** Frequencies of motile and immotile cilia in crown cells (CC) and pit cells (PC)

of embryos at the early headfold (EHF), one-somite, and three-somite stages. Note that ~60% of pit cell cilia are already motile at the early headfold stage (EHF), and *Cerl2* expression in crown cells begins to exhibit L-R asymmetry shortly after EHF, at the late headfold stage (*9*). Bars represent ± SEM.

Figure S11. Ability of mutant forms of Pkd2 to rescue L-R defects of *Pkd2*$^{-/-}$.

Asymmetric expression of *Nodal* in the LPM of *Pkd2*$^{-/-}$ embryos at E8.0 is restored by expression of *Pkd2(R6G)* (top left) but not by that of *Pkd2(R6G, G819X)::Venus* (middle) or *Pkd2(D509V)::Venus* (right). Scale bar, 500μm. Crown cell-specific expression of transgenes in *Pkd2*$^{+/+}$ embryo was confirmed by X-gal staining or *in situ* hybridization for *Venus* (lower panels). Scale bar, 50μm.

Figure S12. Ciliary localization of Pkd2 mutants in LLC-PK1 cells.

(A) Localization of Pkd2(wt)::Venus, Pkd2(D509)::Venus and Pkd2(E442G)::Venus in LLC-PK1 cells. Expression vectors for the indicated protein were transiently expressed in cells, and stained with antibodies to acetylated tubulin (red), Venus (green) and DAPI (blue). Pkd2::Venus distributes to cilia, whereas Pkd2(D509)::Venus and Pkd2(E442G)::Venus fail to be localized to cilia. Scale bar, 5μm. **(B)** The level of Pkd2 expression in the cell lines was examined by Western blot. These cell lines were used to examine Ca^{2+} channel activity (shown in Fig. 4D). Ct, Ct1 and Ct2, control LCC-PK1; A6, F3, M13, K14, #17 and #19 are LCC-PK1 cell lines stably expressing the indicated Pkd2 protein. While LCC-PK1 cells express a low level of endogenous Pkd2, stable cell

lines express a much higher level of exogenous Pkd2.

Figure S13. Interaction of Pkd2(E442G) with Pkd1l1.

HEK293 cells were transfected with the indicated expression vectors. Cell lysates were first incubated with an anti-GFP antibody. Immunoprecipitates were subjected to Western blot analysis with anti-Myc antibody or anti-GFP antibody. Note that GFP-tagged C-terminal Pkd1l1 (45kDa) are co-precipitated with Pkd2-3xMyc and Pkd2(E442G)-3xMyc (113kDa), suggesting that Pkd2(E442G) interacts with Pkd1l1 as wild-type Pkd2(wt) does.

Figure S14. Nodal flow in *Kif3a*$^{-/-}$; *NDE-Kif3a* embryo.

PIV analysis of nodal flow in embryos of the indicated genotypes at E8.0. The color scale indicates the magnitude of the flow (leftward in yellow and red, rightward in blue). Scale bar, 10 μm.

Supplementary Movies

Movie 1. Motility of cilia in the node as visualized by the fluorescence of Pkd2::Venus.

Transgenic embryos that harbor *Foxa2-hsp-Pkd2::Venus* and express Pkd2::Venus protein in pit cells and crown cells were analyzed. Red arrowheads indicate rotating cilia. Note that motile cilia in the node rotate normally.

Movie 2. Motility of cilia in node crown cells at the presomite stage.

Transgenic embryos that harbor *NDE-hsp-Pkd2::Venus* and express Pkd2::Venus protein in crown cells were analyzed at the presomite stage. Fluorescence of Pkd2::Venus was monitored for 10 seconds. Red arrowheads indicate rotating cilia, while blue arrowheads indicate immotile cilia. Note that most of the cilia are immotile.

Movie 3. Motility of cilia in node crown cells at the three-somite stage.

Transgenic embryos that harbor *NDE-hsp-Pkd2::Venus* and express Pkd2::Venus protein in crown cells were analyzed at the three-somite stage. Fluorescence of Pkd2::Venus was monitored for 10 seconds. Red arrowheads indicate rotating cilia, while blue arrowheads indicate immotile cilia.

References

1. H. Sasaki, B. L. Hogan, *Genes Cells* **1**, 59 (1996).
2. Y. Nishizaki, K. Shimazu, H. Kondoh, H. Sasaki, *Mech Dev* **102**, 57 (2001).
3. T. Nagai *et al.*, *Nat Biotechnol* **20**, 87 (2002).
4. H. Adachi *et al.*, *Genes Dev* **13**, 1589 (1999).
5. D. P. Norris, E. J. Robertson, *Genes Dev* **13**, 1575 (1999).
6. Y. Imai, Y. Matsushima, T. Sugimura, M. Terada, *Nucleic Acids Res* **19**, 2785 (1991).
7. P. Pennekamp *et al.*, *Curr Biol* **12**, 938 (2002).
8. S. Marques *et al.*, *Genes Dev* **18**, 2342 (2004).
9. A. Kawasumi *et al.*, *Dev Biol* **353**, 321 (2012).
10. M. Hashimoto *et al.*, *Nat Cell Biol* **12**, 170 (2011).
11. K. Shinohara *et al.*, *Meas Sci Technol* **15**, 1965 (2004).

12. P. Koulen *et al.*, *Nat Cell Biol* **4**, 191 (2002).
13. S. Mizushima, S. Nagata, *Nucleic Acids Res* **18**, 5322 (1990).
14. S. Field *et al.*, *Development* **138**, 1131 (2011).
15. S. Nonaka, H. Shiratori, Y. Saijoh, H. Hamada, *Nature* **418**, 96 (2002).
16. T. Nakamura *et al.*, *Dev Cell* **11**, 495 (2006).

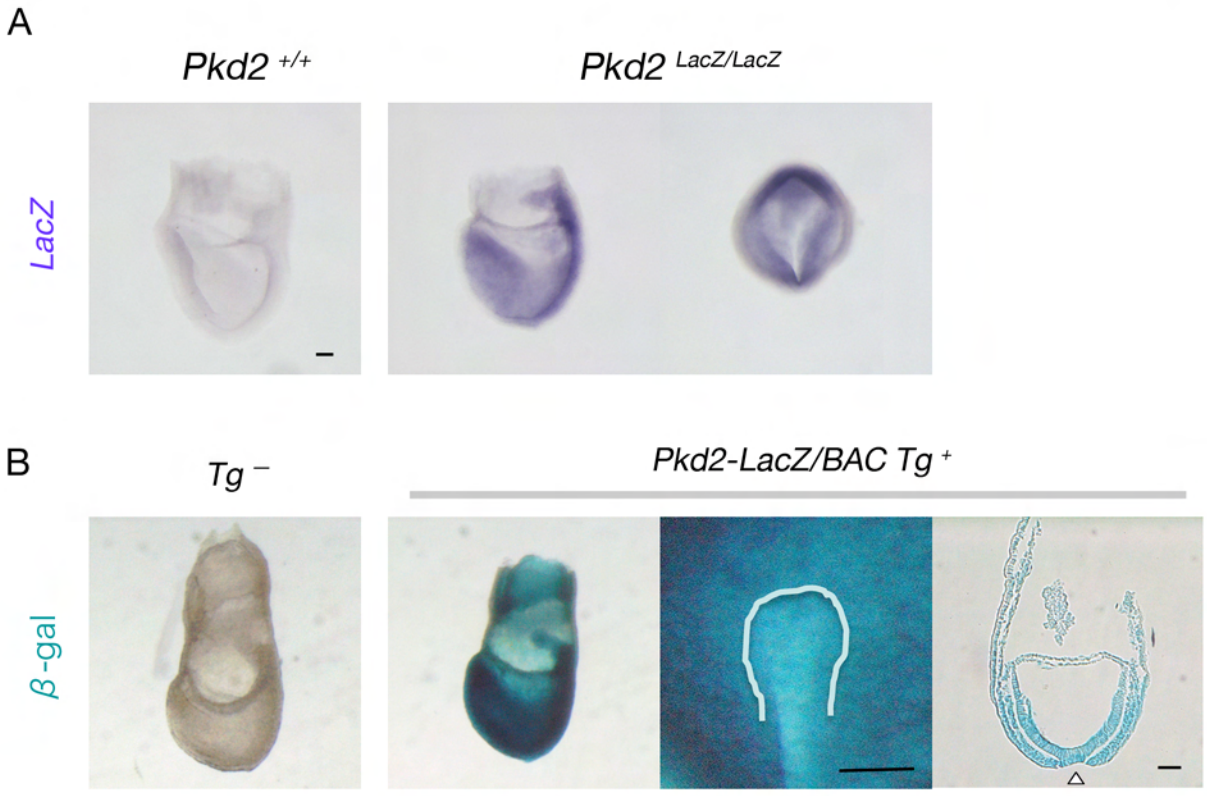
A
Pkd2 +/+
Pkd2 LacZ/LacZ
LacZ
B
Tg −
Pkd2-LacZ/BAC Tg +
β-gal

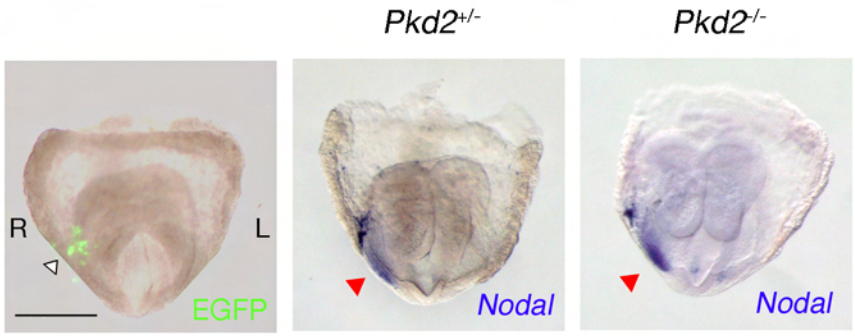
Pkd2+/-
Pkd2-/-
R
L
EGFP
Nodal
Nodal

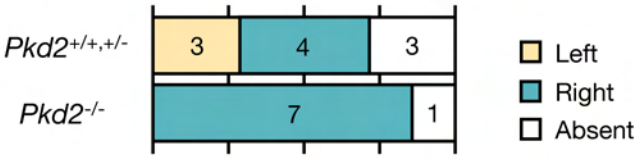
Pkd2+/+,+/-
Pkd2-/-
3
4
3
7
1
Left
Right
Absent

A

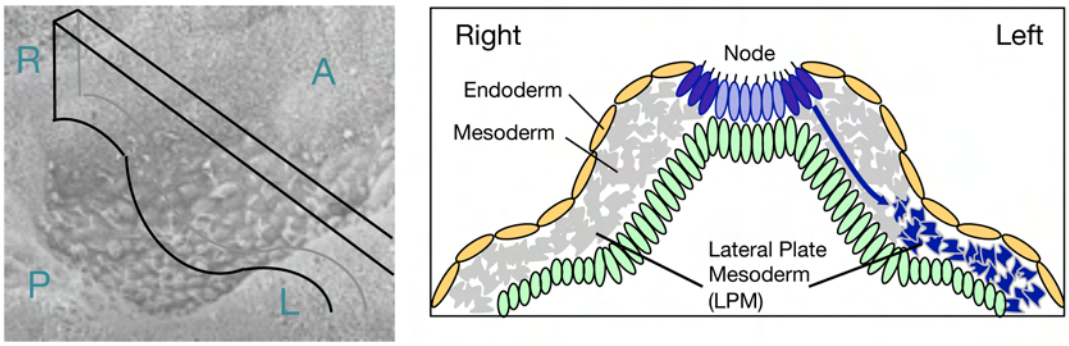
R
A
P
L
Right
Left
Node
Endoderm
Mesoderm
Lateral Plate
Mesoderm
(LPM)

B

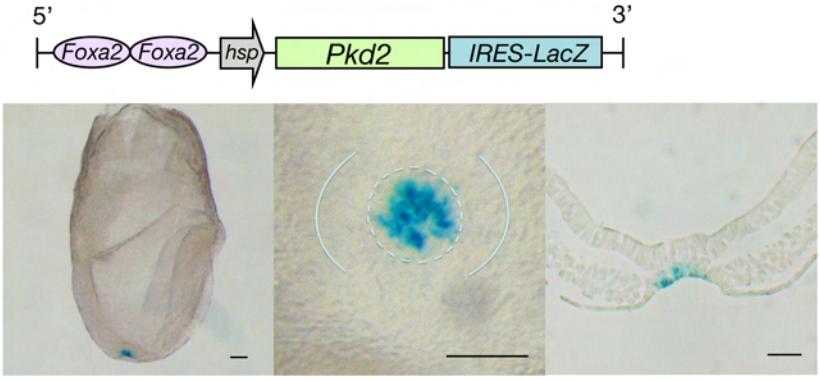
5'
3'
Foxa2
Foxa2
hsp
Pkd2
IRES-LacZ

C

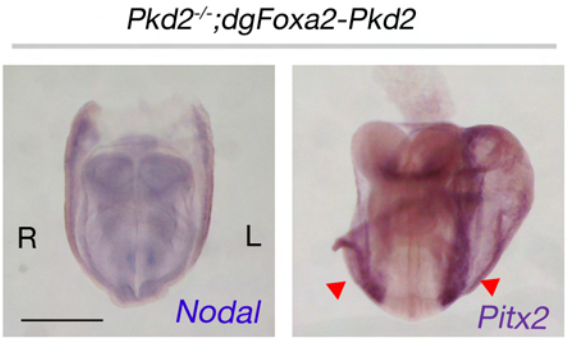
Pkd2-/-;dgFoxa2-Pkd2
R
L
Nodal
Pitx2

D

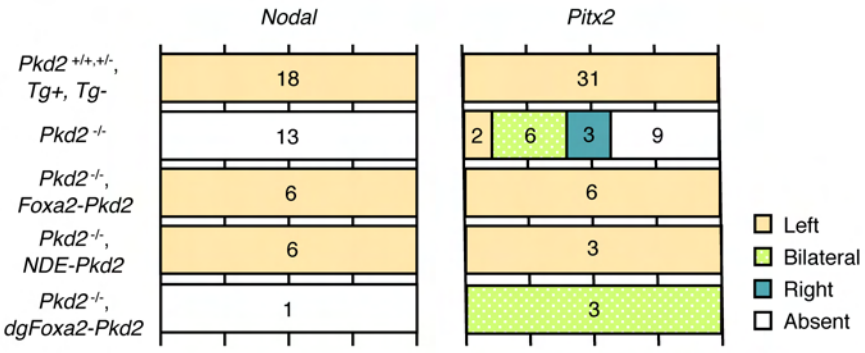
Nodal
Pitx2
Pkd2 +/+,+/-, Tg+, Tg-
Pkd2 -/-
Pkd2 -/-, Foxa2-Pkd2
Pkd2 -/-, NDE-Pkd2
Pkd2 -/-, dgFoxa2-Pkd2
18
13
6
6
1
31
2
6
3
9
6
3
3
Left
Bilateral
Right
Absent

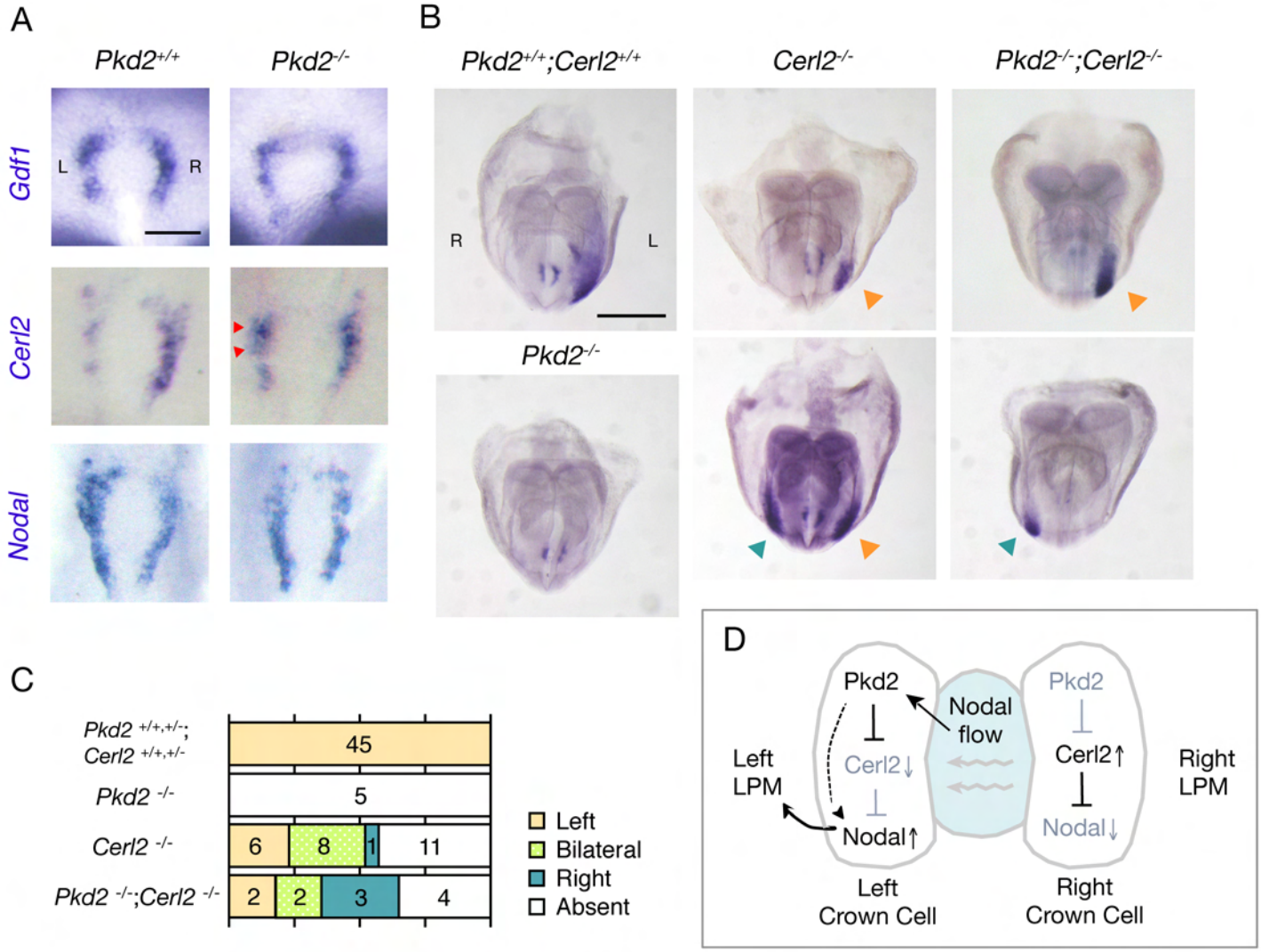
A
Pkd2+/+
Pkd2-/-
Gdf1
Cerl2
Nodal
L
R
B
Pkd2+/+;Cerl2+/+
Cerl2-/-
Pkd2-/-;Cerl2-/-
Pkd2-/-
R
L
C
Pkd2 +/+,+/-; Cerl2 +/+,+/-
Pkd2 -/-
Cerl2 -/-
Pkd2 -/-;Cerl2 -/-
45
5
6
8
1
11
2
2
3
4
Left
Bilateral
Right
Absent
D
Pkd2
Nodal flow
Pkd2
Left LPM
Cerl2↓
Cerl2↑
Right LPM
Nodal↑
Nodal↓
Left Crown Cell
Right Crown Cell

Pkd2$^{+/+}$

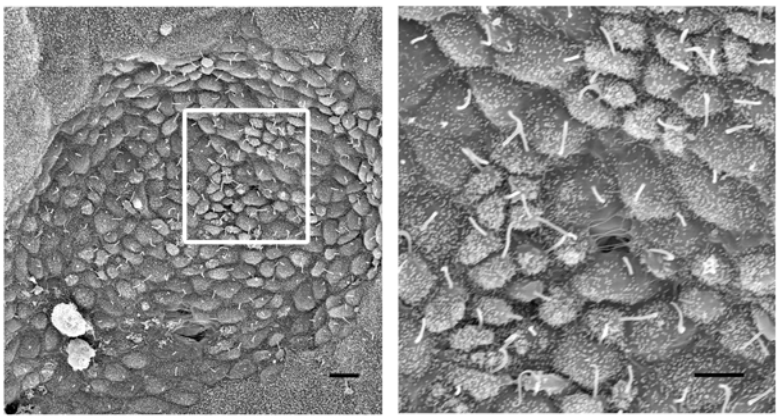

Pkd2$^{-/-}$

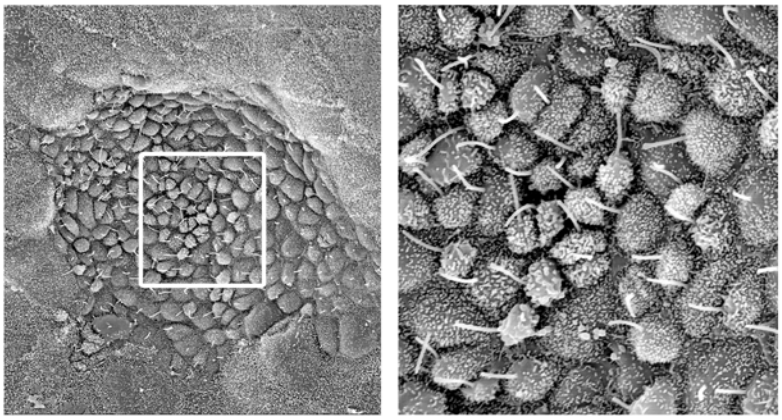

yoshibafigS6

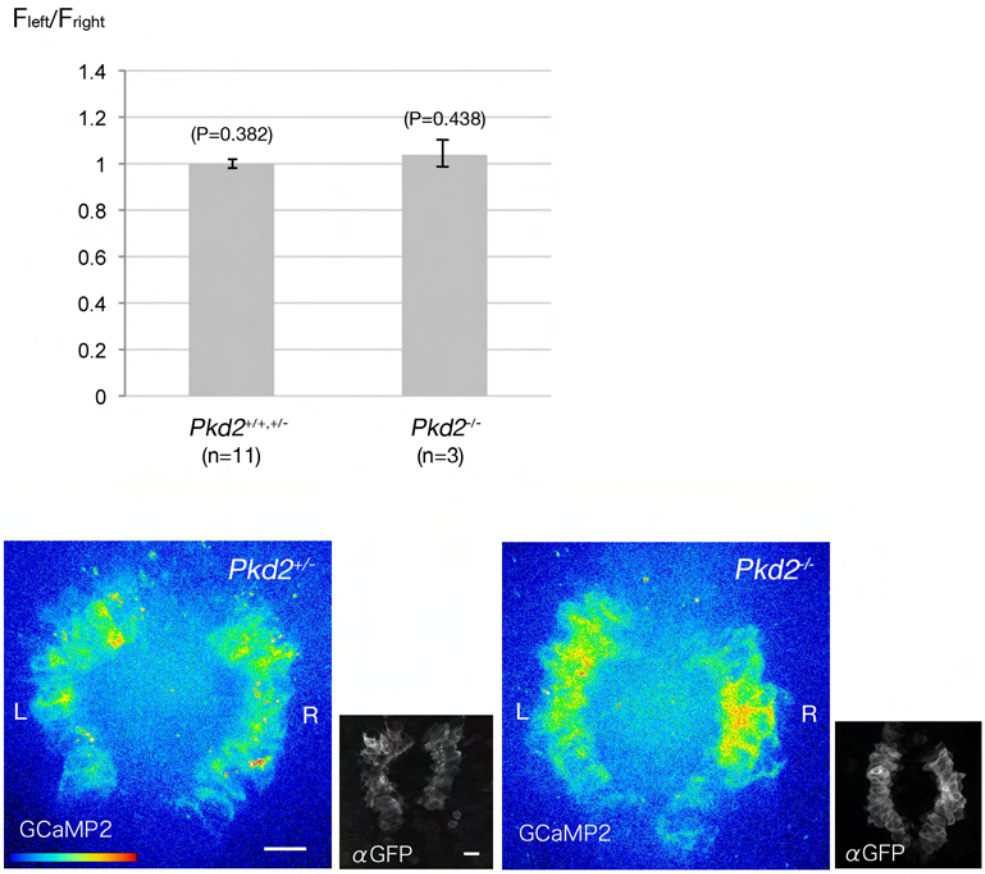

yoshibafigS7

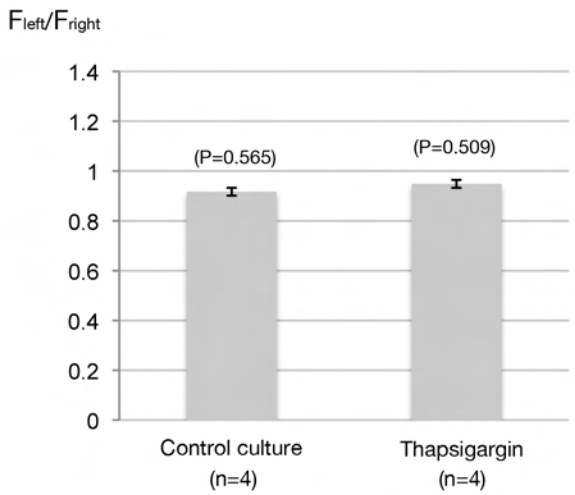

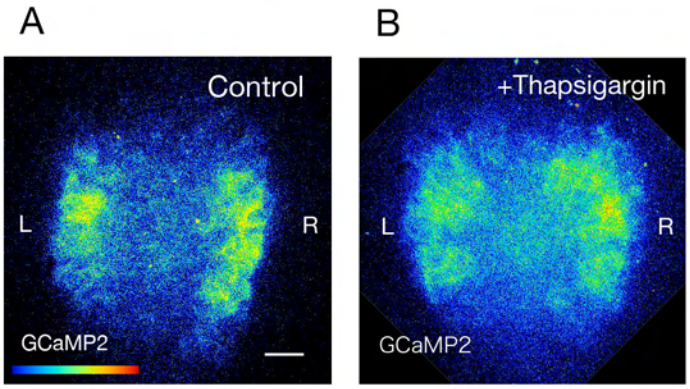

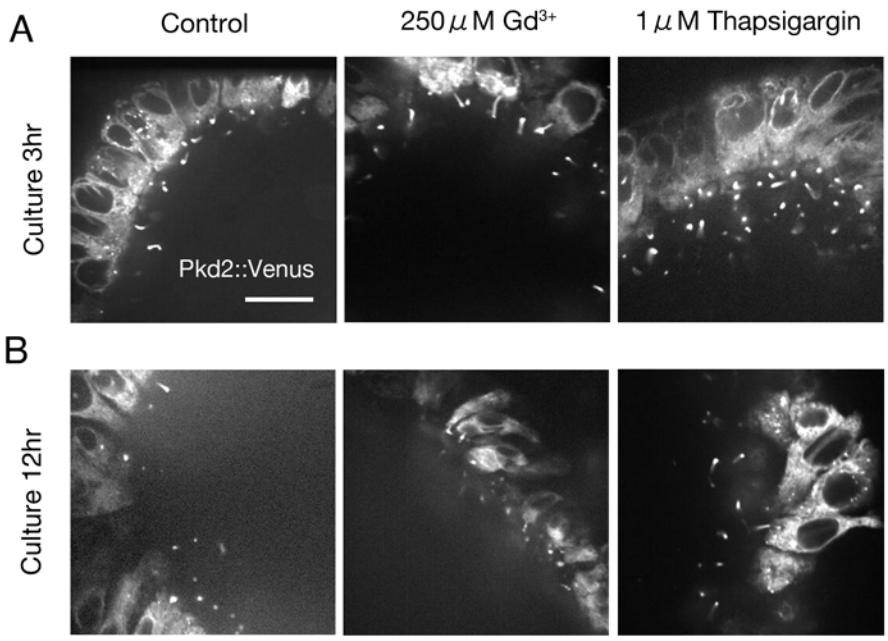
A
Control
250 μM Gd3+
1 μM Thapsigargin
Culture 3hr
Pkd2::Venus
B
Culture 12hr

A

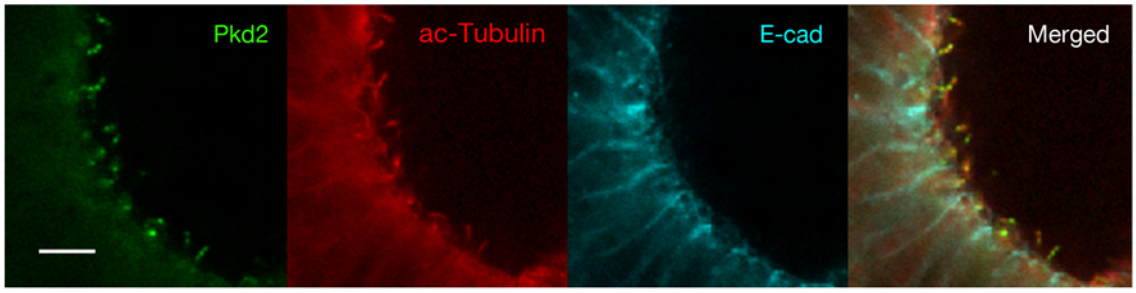
Pkd2
ac-Tubulin
E-cad
Merged

B

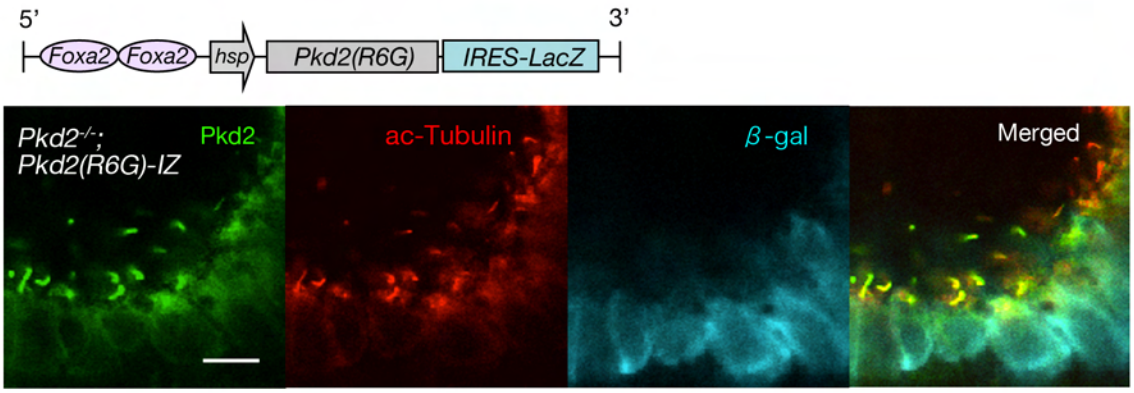
5'
3'
Foxa2
Foxa2
hsp
Pkd2(R6G)
IRES-LacZ
Pkd2-/-;
Pkd2(R6G)-IZ
Pkd2
ac-Tubulin
β-gal
Merged

C

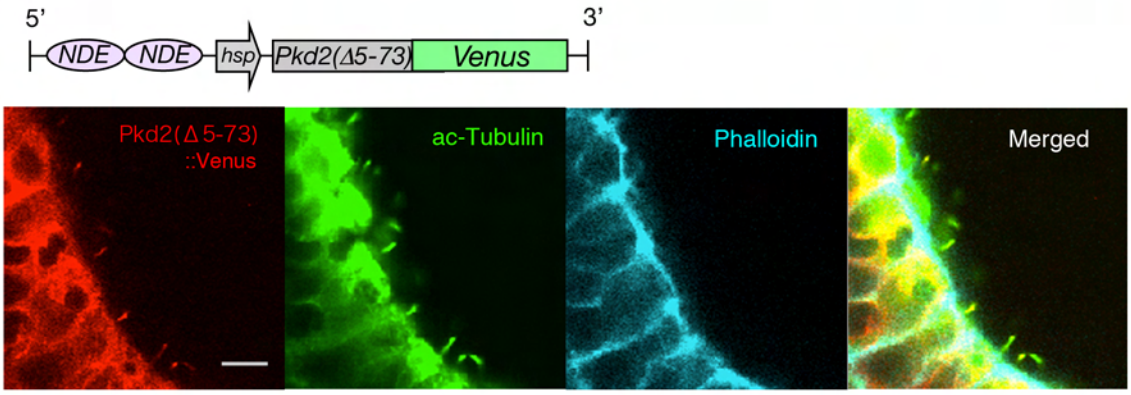
5'
3'
NDE
NDE
hsp
Pkd2(Δ5-73)
Venus
Pkd2(Δ5-73)
::Venus
ac-Tubulin
Phalloidin
Merged

D

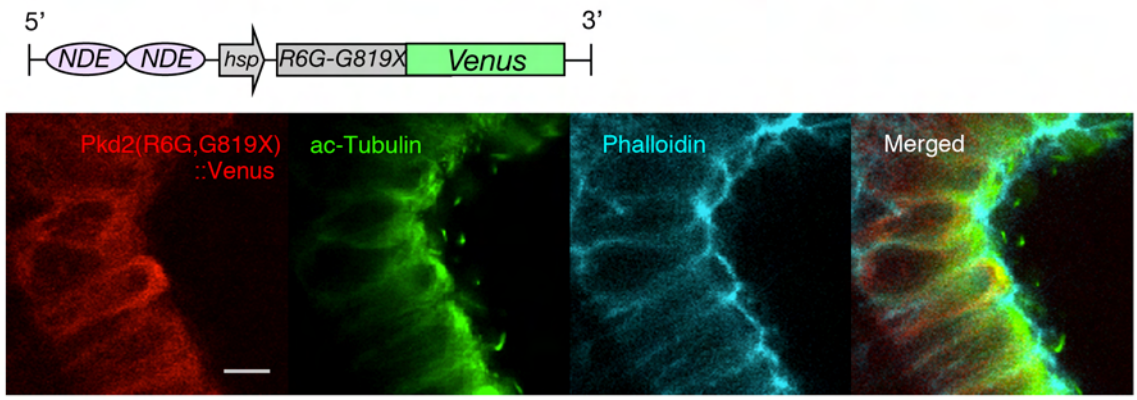
5'
3'
NDE
NDE
hsp
R6G-G819X
Venus
Pkd2(R6G,G819X)
::Venus
ac-Tubulin
Phalloidin
Merged

A

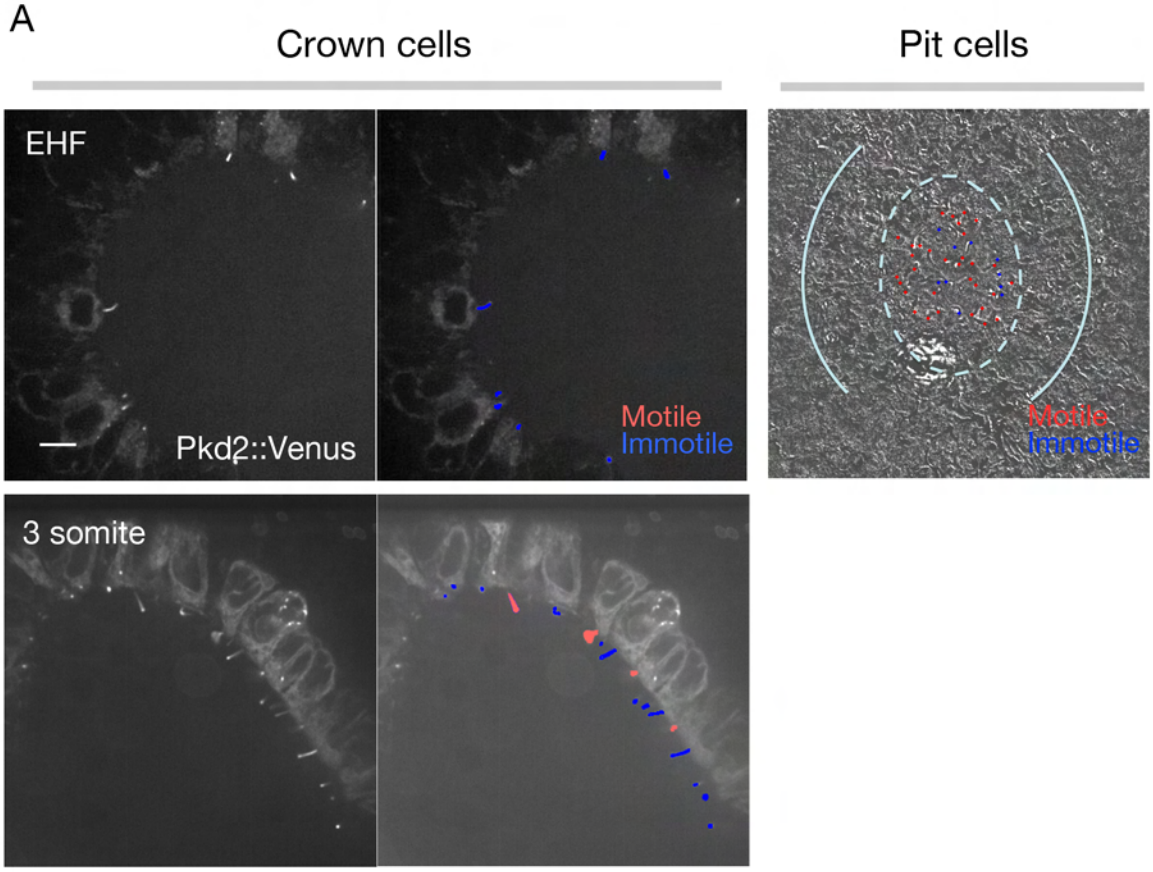
Crown cells
Pit cells
EHF
Pkd2::Venus
Motile
Immotile
Motile
Immotile
3 somite

B

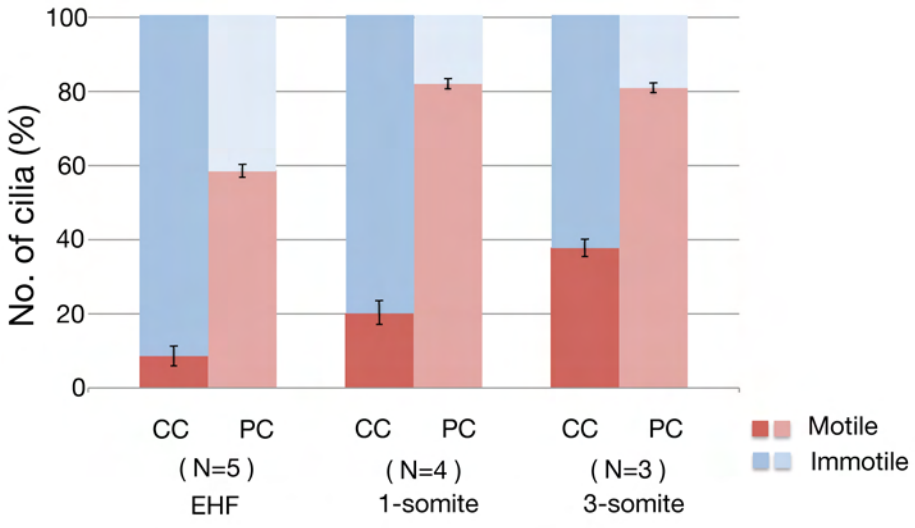
No. of cilia (%)
100
80
60
40
20
0
CC
PC
(N=5)
EHF
CC
PC
(N=4)
1-somite
CC
PC
(N=3)
3-somite
Motile
Immotile

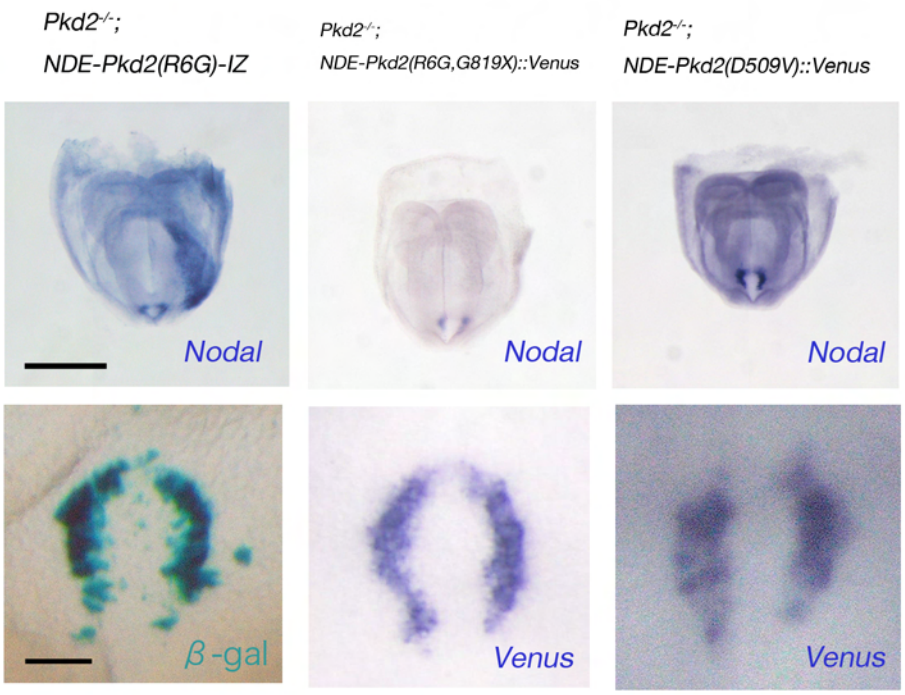
Pkd2-/-;
NDE-Pkd2(R6G)-IZ
Pkd2-/-;
NDE-Pkd2(R6G,G819X)::Venus
Pkd2-/-;
NDE-Pkd2(D509V)::Venus
Nodal
Nodal
Nodal
β-gal
Venus
Venus

A

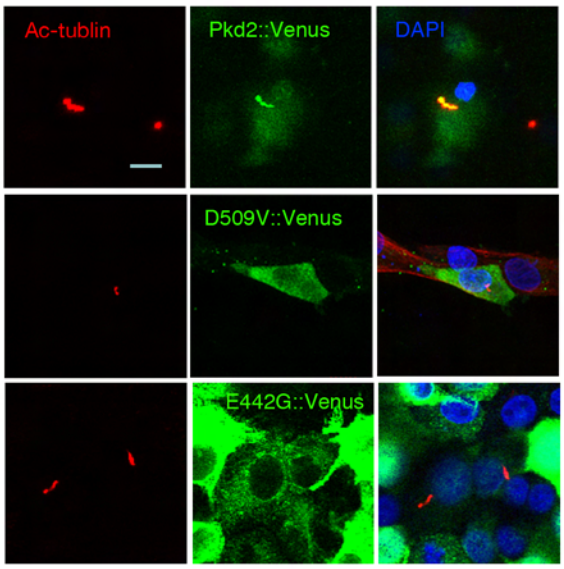
Ac-tublin
Pkd2::Venus
DAPI
D509V::Venus
E442G::Venus

B

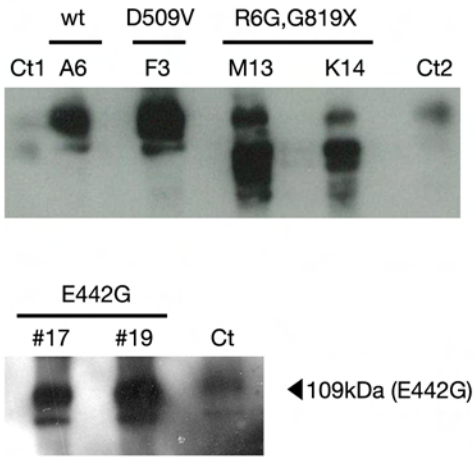
wt
D509V
R6G,G819X
Ct1
A6
F3
M13
K14
Ct2
◀109kDa (wt, D509V)
◁ 95kDa (R6G,G819X)
E442G
#17
#19
Ct
◀109kDa (E442G)

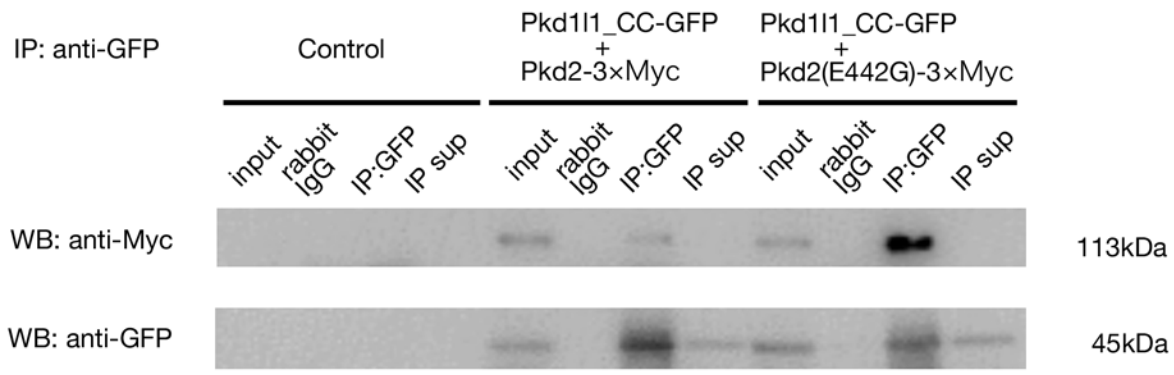
IP: anti-GFP
Control
Pkd1l1_CC-GFP + Pkd2-3×Myc
Pkd1l1_CC-GFP + Pkd2(E442G)-3×Myc
input
rabbit IgG
IP:GFP
IP sup
input
rabbit IgG
IP:GFP
IP sup
input
rabbit IgG
IP:GFP
IP sup
WB: anti-Myc
113kDa
WB: anti-GFP
45kDa

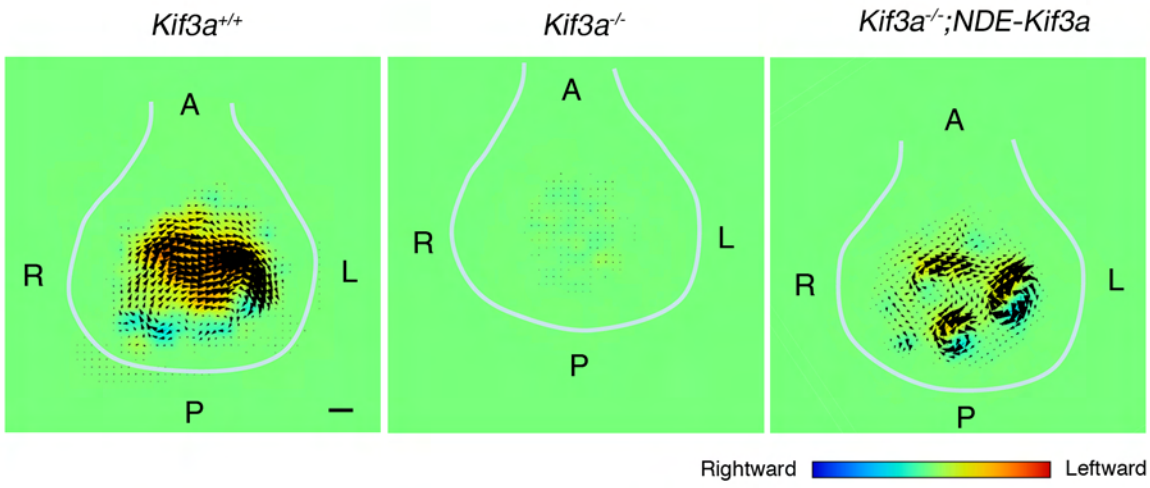
Kif3a+/+
Kif3a-/-
Kif3a-/-;NDE-Kif3a
A
R
L
P
Rightward
Leftward